

Variable Importance of Macrofaunal Functional Biodiversity for Biogeochemical Cycling in Temperate Coastal Sediments

U. Braeckman,^{1*} M. Yazdani Foshtomi,^{1,2} D. Van Gansbeke,¹
F. Meysman,^{3,4} K. Soetaert,³ M. Vincx,¹ and J. Vanaverbeke¹

¹Marine Biology Research Group, Department of Biology, Ghent University, Krijgslaan 281/S8, 9000 Ghent, Belgium; ²Iranian National Institute for Oceanography, 9, Etemadzadeh Avenue, West Fatemi Street, Tehran, Iran; ³Department of Ecosystem Studies, Netherlands Institute for Sea Research, PO Box 140, 4400 AC Yerseke, The Netherlands; ⁴Department of Analytical and Environmental Chemistry, Vrije Universiteit Brussel (VUB), Pleinlaan 2, 1050 Brussels, Belgium

ABSTRACT

Coastal marine systems are currently subject to a variety of anthropogenic and climate-change-induced pressures. An important challenge is to predict how marine sediment communities and benthic biogeochemical cycling will be affected by these ongoing changes. To this end, it is of paramount importance to first better understand the natural variability in coastal benthic biogeochemical cycling and how this is influenced by local environmental conditions and faunal biodiversity. Here, we studied sedimentary biogeochemical cycling at ten coastal stations in the Southern North Sea on a monthly basis from February to October 2011. We explored the spatio-temporal variability in oxygen consumption, dissolved inorganic nitrogen and alkalinity fluxes, and estimated rates of nitrification and denitrification from a mass budget. In a next step, we statistically modeled their relation with environmental variables

and structural and functional macrobenthic community characteristics. Our results show that the cohesive, muddy sediments were poor in functional macrobenthic diversity and displayed intermediate oxygen consumption rates, but the highest ammonium effluxes. These muddy sites also showed an elevated alkalinity release from the sediment, which can be explained by the elevated rate of anaerobic processes taking place. Fine sandy sediments were rich in functional macrobenthic diversity and had the maximum oxygen consumption and estimated denitrification rates. Permeable sediments were also poor in macrobenthic functional diversity and showed the lowest oxygen consumption rates and only small fluxes of ammonium and alkalinity. Macrobenthic functional biodiversity as estimated from bioturbation potential appeared a better variable than macrobenthic density in explaining oxygen consumption, ammonium and alkalinity fluxes, and estimated denitrification. However, this importance of functional biodiversity was manifested particularly in fine sandy sediments, to a lesser account in permeable sediments, but not in muddy sediments. The strong relationship between macrobenthic functional biodiversity and biogeochemical cycling in fine sandy sediments implies that a future loss of macrobenthic functional diversity will have important repercussions for benthic ecosystem functioning.

Received 13 November 2013; accepted 28 January 2014

Electronic supplementary material: The online version of this article (doi:10.1007/s10021-014-9755-7) contains supplementary material, which is available to authorized users.

Author contributions: UB, JV, and KS conceived of or designed study. UB, MYF, DVG, and JV performed research. UB, JV, and KS analyzed data. UB contributed new methods or models. UB, JV, FM, KS, and MV wrote the paper.

*Corresponding author; e-mail: ulrike.braeckman@ugent.be

Key words: benthic ecosystem functioning; macrobenthos; functional biodiversity; oxygen consumption; nutrient fluxes; alkalinity; North Sea; bioturbation potential.

INTRODUCTION

Coastal seas cover only 10 % of the total ocean surface (Jørgensen 1983; Smith and Hollibaugh 1993; Wollast 1998) but provide a wealth of ecosystem goods and services including carbon storage or nutrient availability. The world-wide human pressures on coastal ecosystems (Vitousek and others 1997; Halpern and others 2008) make understanding and predicting the effects of human and climate-change-induced stressors on coastal marine ecosystems nowadays one of the main challenges (Doney 2010).

Owing to intensive primary production and shallow water depth, a close coupling generally exists between the pelagic and benthic compartments in coastal ecosystems (for example, Marcus and Boero 1998). The biogeochemical cycling of elements within coastal sediments influences water column processes in multiple ways. For example, primary production and associated phytoplankton dynamics in the water column are crucially dependent on the rate and timing of nutrient release during benthic organic matter (OM) mineralization (Lancelot and others 2005; Soetaert and Middelburg 2009). Also, anaerobic pathways of benthic mineralization can be an important source of alkalinity generation, which increase the capability of CO₂ uptake in coastal waters (Chen 2002; Thomas and others 2009; Hu and Cai 2011). So an important challenge is to predict how benthic biogeochemical cycling in coastal seas will be affected by anthropogenic and climate-change-induced pressures.

In addition to being sites of intense OM mineralization, coastal sediments are also typically inhabited by a rich faunal community, which can exert an important control on sedimentary biogeochemical cycling through their bioturbation and bio-irrigation activities (Aller 1988; Meysman and others 2006). In search for food, these organisms actively rework and irrigate the sediment matrix. Oxygen and OM are transported into the deeper sediment layers, while the exchange of solutes between pore water and overlying water is enhanced by various burrow flushing activities (Yingst and Rhoads 1980; Mermillod-Blondin and others 2004). This increases nutrient turnover, and hence, replenishes the nutrient pool available for primary production (Blackburn 1988). Given the

variety in macrobenthic sediment reworking activities (Gérino and others 2003), it is rather the functional biodiversity than taxonomic biodiversity that matters for benthic ecosystem functioning (Emmerson and Raffaelli 2000; Ieno and others 2006; Cardinale and others 2012).

The relation between functional biodiversity and biogeochemical cycling in marine sediments has mainly been assessed through manipulative experiments in a laboratory context (Mermillod-Blondin and others 2004; Waldbusser and others 2004; Michaud and others 2005; Ieno and others 2006; Norling and others 2007; Godbold and others 2008; Braeckman and others 2010; Bulling and others 2010; Gilbertson and others 2012). This experimental approach is suitable to examine the effect of a single species or a multispecies assemblage on biogeochemical cycling. The advantage is that possible cause-effect relationships can be uncovered, without the inherently co-varying environmental factors operating in the real world (Benton and others 2007). However, the upscaling of these experimentally derived functional biodiversity-ecosystem functioning relationships to the field situation is difficult because the artificial assemblages used in laboratory experiments are highly simplified models of the in situ community. In addition, experiments are typically only of short duration, whereas the sediment is often strongly manipulated and artifacts may arise (for example, container effects). As an alternative to experimental studies, one can carry out in situ observational studies that make use of proxies for functional biodiversity and/or ecosystem functioning. One such proxy is the bioturbation potential of the community (BPC), an index that involves biomass, abundance, and functional sediment reworking characteristics, as a measure for macrobenthic functional biodiversity (Solan and others 2004). BPC was negatively related to total organic carbon and positively to chlorophyll concentrations in the sediment (Solan and others 2012) and positively to the apparent redox potential discontinuity layer (aRPD) as derived from sediment profile imaging (Birchenough and others 2012). This aRPD was calculated as the mean depth at which the sediment changes color (from light colored to black), and was interpreted as a proxy for the intensity of biogeochemical cycling in the sediment. However, the aRPD is the result of a combination of environmental conditions, food input and faunal activity (Teal and others 2010), and so, to relate macrobenthic functional biodiversity *independently* to benthic carbon cycling, it is therefore better to use actual measurements of biogeochemical cycling

(Van Colen and others 2012). Because of the strong influence of the annual phytoplankton bloom on biogeochemical cycling in coastal seas, such relationships should be investigated over a full seasonal cycle (Teal and others 2010; Provoost and others 2013).

In the light of sustainable ecosystem management and associated monitoring, it is important to understand how OM mineralization and nutrient release are distributed in space and time and how this carbon mineralization relates to the predominant environmental conditions and local biodiversity. Few attempts have been made to assess the relative importance of functional biodiversity and environmental conditions in affecting biogeochemical processes in natural systems because these ecosystems are structured by multiple and simultaneously operating abiotic and biotic factors that are difficult to disentangle (Godbold and Solan 2009). In this study, we therefore measured various biogeochemical processes at ten stations in the Southern North Sea over a yearly cycle. These sites are representative of a range of sediment types and macrobenthic communities. We tested for (1) spatial and (2) temporal differences in biogeochemical cycling and functional biodiversity of macrobenthos. Further, we (3) developed models to predict oxygen, ammonium, and alkalinity fluxes, nitrification and denitrification from environmental variables including functional biodiversity (that is, bioturbation potential) of macrobenthos.

MATERIALS AND METHODS

Our approach involved a combination of field measurements and modeling. During monthly sampling campaigns, we quantified rates of sedimentary biogeochemical cycling, environmental parameters, and functional biodiversity at ten stations in the Southern North Sea with varying sediment types and contrasting macrobenthic communities. This sampling strategy covered the most significant temporal and spatial variability in environmental parameters, functional biodiversity, and rates of sedimentary biogeochemical cycling in the study area. As rates of sedimentary biogeochemical cycling, we quantified sediment community oxygen consumption (SCOC), the exchange of dissolved inorganic nitrogen (DIN) and alkalinity (A_T) across the sediment–water interface. These fluxes were obtained by incubating undisturbed sediment cores. From the resulting oxygen and DIN fluxes, we modeled nitrification and potential denitrification rates using an integrated mass bud-

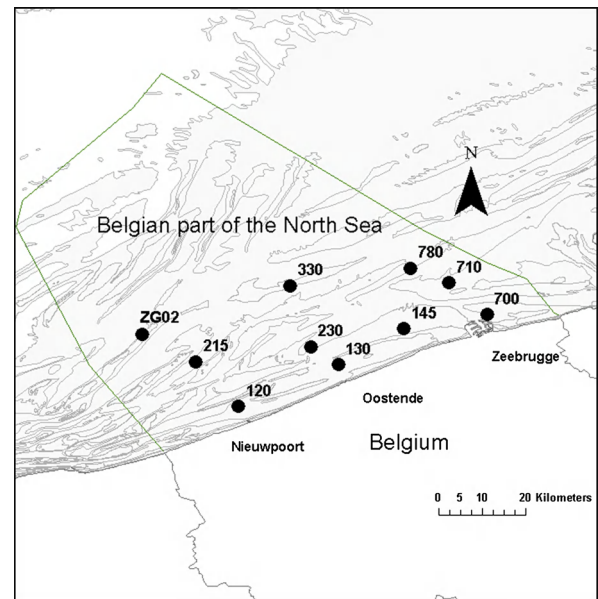


Figure 1. Bathymetry map of the Belgian part of the North Sea with indication of the sampled stations. Stations 215, ZG02 have been sampled only in June and August. 330 was sampled in June, August, and October (330).

get approach (Soetaert and others 2001; Braeckman and others 2010). We quantified functional biodiversity as community bioturbation potential (BPC, Solan and others 2004).

Sampling

SCOC, DIN, and A_T fluxes were quantified at seven stations (station codes: 120, 130, 230, 145, 700, 710, and 780) on a monthly basis from February to September 2011 (Figure 1; Appendix A in Electronic Supplementary Material) with the *RV Zeeleeuw*. Three additional stations with coarse sediment (ZG02, 330, and 215) were sampled in June and August 2011. In October 2011, two representative fine sandy stations (130 and 780) and one representative coarse sandy station (330) were sampled for measurements of denitrification ($N_2:Ar$ method, see below) and DIC flux.

At each station, a CTD cast was performed and the bottom water (± 1 m above the sea floor) was sampled with 5-L Niskin bottles. The bottom water was subsampled for oxygen (duplicate 12 ml Winkler bottles) and DIN concentrations (triplicate 10 ml in scintillation vials, samples filtered on Whatman™ GF/F filters). Three additional water samples were filtered on precombusted Whatman™ GF/F filters for the determination of pigments (chl-*a* and its degradation products).

Sediment Core Incubations

At the seven stations (120, 130, 230, 145, 700, 710, and 780), triplicate small sediment cores (Plexiglass, internal diameter \varnothing : 10 cm; H : 25 cm) were inserted in a Reineck Box corer that was deployed several times. A 3-ml sediment subsample of the upper 2 cm of the sediment was used for the determination of pigments (in triplicate) and was stored at -80°C until analysis.

At the three additional coarse sediment stations (330, 215, and ZG02), we used centrally stirred chambers (Plexiglass \varnothing : 19 cm; H : 30 cm) to create an advective pore water flow (Huettel and Rush 2000). At each station, three chambers were filled up to 10 cm with homogenized sediment from the upper 10 cm of the sediment obtained from a Reineck box corer.

Cores were transported within 10 h to a temperature-controlled room at in situ temperature (recorded from the CTD cast) in the lab and immediately submerged in well-aerated sea water. This water is further referred to as "tank water." Teflon-coated magnets rotated by a central magnet were adjusted 5 cm above the sediment surface of the small cores (\varnothing : 10 cm) to ensure mixing of overlying water. The rate of water circulation was kept well below the resuspension threshold. The centrally stirred chambers had top lids equipped with a flat stirring disk, which was positioned at 5.4 cm above the sediment surface and rotated at 12 rpm. The sediments were left to acclimatize overnight in the dark.

The next day, closed sediment incubations were initiated by closing cores airtight. Cores were subsequently incubated in the dark for a period long enough for the fluxes to reach steady-state but ensuring oxygen did not drop below 50 % saturation. The actual incubation period depended on the sediment type and temperature (that is, longer incubation times for coarse sediment and measurements at low temperatures). From April onward, the influence of water column processes was estimated by incubating tank water in cores of half the volume of a normal fine sandy sediment core (that is, internal diameter \varnothing : 10 cm; H : 12.5 cm). The overlying water in all incubations was subsampled with a glass syringe for O_2 (2×12 ml, Winkler), DIN (3×10 ml), and A_T (3×25 ml), the latter two subsamples filtered through Whatman™ GF/F filters. Oxygen and alkalinity concentrations were determined at the start and the end of the incubation, because their respective decrease and increase are generally linear. Triplicate DIN

samples were taken at the start and end of the incubation, as well as half way through the incubation time to check for linearity in DIN exchange. At the same time, samples of tank water were taken for O_2 , DIN, and A_T to correct for concentration changes due to water replacement during subsampling. Oxygen samples were stored in the same temperature-controlled room in the dark until further analysis (within 3 days); DIN samples were stored frozen (-20°C); and alkalinity samples were stored refrigerated (4°C).

For the N_2 :Ar samples in October, all equipment was stored submerged in the incubation tank 48 h before samples were obtained, to avoid introduction of new surfaces for O_2 , N_2 , and Ar adsorption. This is pivotal for the correct determination of N_2 production (Kana and others 1994). Sample collection was performed as described in Na and others (2008). The concentrations of N_2 and Ar were determined by membrane-inlet mass spectrometry (MIMS; GAM; IPI) at the Max Planck Institute for Marine Microbiology in Bremen. DIC samples were analyzed with a Li-Cor® LI 7000 solid state infrared CO_2 detector after acidification (AS-C3 DIC analyzer, Apollo SciTech).

At the end of the incubations, the cores were opened and aerated again. After 24 h of reaeration, depth profiles of oxygen were measured in the sediment with O_2 microsensors (25 and 100 μm tip size, Unisense) in vertical increments of 250 μm (3 replicate profiles in each core). pH depth profiles were also measured using a sturdy pH sensor (Hannah Instruments) in February–May at 1-cm depth intervals down to 10 cm. Hereafter, the sediment surface (upper 2 cm) was subsampled (2 ml) for the analysis of pigments, % organic carbon and nitrogen and grain size. Subsequently, the remainder of the sediment was sieved on a 1-mm mesh to sample the macrofauna, which was preserved in ethanol. The pigment samples were stored at -80°C until analysis, whereas the organic C/N and grain size samples were oven-dried at 60°C before analysis.

Macrobenthos Analysis

Macrobenthos specimens were identified to the lowest possible taxonomic level (typically species level) and biomasses were determined (blotted wet weights). Using this macrofauna dataset, the bio-turbation potential index (BP_i) and the BPC were calculated (Solan and others 2004; Birchenough and others 2012; Queirós and others 2013).

Laboratory Analyses and Flux Calculation

Pigments were determined by HPLC analysis according to Wright and Jeffrey (1997). Total organic C and N content was analyzed with a FLASH 2000 NC Elemental Analyzer (0.01 % detection limit) and sediment granulometry by laser diffraction (Malvern Instruments, 2 μm detection limit). Sediment permeability was calculated according to Hazen ($k_H = 1.1019 \times 10^3 \text{ m}^{-2} \text{ s} * d_{10}^2 * v$; with k_H = permeability; d_{10} = first decile of the grain size distribution (m); and v = kinematic viscosity (in $\text{m}^2 \text{ s}^{-1}$)) (Eggleston and Rojstaczer 1998). Obtained permeabilities were corrected according to Rusch and others (2001). Sediments with a k_H above $2.5 \times 10^{-12} \text{ m}^2$ are considered permeable (Forster and others 2003; Wilson and others 2008).

Oxygen was analyzed by automated Winkler titration (Parsons and others 1984; detection limit $\sim 2 \mu\text{mol l}^{-1}$), DIN was analyzed using automated colorimetric techniques (SKALAR) and alkalinity was determined by automated end-point titration (to pH 4.2) (G20 Mettler-Toledo). Oxygen and alkalinity fluxes were calculated from the difference between initial and final concentrations in the overlying water compensating for concentration changes during subsampling. DIN, $\text{N}_2\text{:Ar}$, and DIC fluxes were calculated, after correction for dilution by refill water, from the significant regression slopes ($P < 0.05$) of concentration over time. Finally, a correction for the processes occurring in the water column was made in the fine sandy sediment cores from April to October, by subtracting the rates in the water column from the total measured rate.

Mass Budget Modeling

The fluxes of O_2 , NO_x , and NH_x across the sediment-water interface were used to estimate rates of denitrification, nitrification, and total carbon and nitrogen mineralization. This was done by constructing an integrated mass balance of oxygen, nitrate, and ammonium over the entire sediment column (Soetaert and others 2001). See Appendix B in Electronic Supplementary Material for detailed methodology.

It must be noted that the DIN concentrations of the "tank water" used in the core incubations (see further) differed from the field DIN concentrations (see Appendix C in Electronic Supplementary Material): although NH_x concentrations were rather similar in the field and in the lab, NO_x concentrations were one order of magnitude higher in the tank than in the field. The reported NO_x

fluxes and modeled denitrification estimates should therefore be considered as "potential rates."

Statistical Analyses

Two-way ANOVAs with type III sums of squares for unbalanced designs, followed by Tukey post-hoc tests were carried out to investigate whether the variation in environmental variables, univariate macrobenthic measures (species density, richness, biomass, BPC), and measured fluxes (SCOC, DIN, and alkalinity fluxes) and modelled processes (nitrification, denitrification) and modelled processes (nitrification, denitrification) depended on the categorical predictors station and month and their interaction station * month. To ensure homogeneity of variances, some variables were square-root transformed (Table 1). Multivariate differences in macrobenthic communities among station and month were tested with a two-way-crossed ANOSIM. Subsequent SIMPER analysis indicated the macrobenthic species that contributed most to the community composition of each station.

Second, we constructed linear models to predict SCOC, NH_x , and alkalinity fluxes and estimated denitrification and nitrification, as a function of the abiotic and biotic (macrobenthic) environmental variables. Only uncorrelated environmental variables were selected, based on the variance inflation factor less than 5 (Heiberger and Holland 2004): median grain size, rather than silt percentage, macrobenthic density rather than species richness and biomass, water column chl- a , N and C in the sediment, temperature, and BPC. Graphical exploratory techniques were used to check the assumptions for linear regression prior to analysis. However, plots of residuals versus fitted values clearly indicated heterogeneity of variances. Therefore, we adopted a linear regression with a generalized least-squares extension (West and Welch 2006; Pinheiro and Bates 2009; Zuur and others 2009), which allows unequal variances among treatment combinations to be modeled as a variance covariance matrix (West and Welch 2006; Pinheiro and Bates 2009). Following West and Welch (2006) and Zuur and others (2009), the most appropriate variance covariate matrix was determined using AIC scores in conjunction with plots of fitted values versus residuals with different variance covariate terms relating to the independent variables, using restricted maximum likelihood (ML) (REML, West and Welch (2006)). This procedure resulted in the use of a variance structure that allowed for different variances per stratum for station (varIdent function, R package nlme). Violation of independence of the residuals through temporal

Table 1. Results of ANOVA for Water Column and Sediment Characteristics, Fluxes, and Macrobenthic Descriptors

Variable	Factor	<i>F</i>	df _{term}	df _{error}	<i>P</i>	Transformation
Water chl- <i>a</i>	St * M	8.42	36	110	***	√
Sediment chl- <i>a</i>	St * M	18.54	34	103	***	√
Median grain size	St * M	1.89	36	110	**	
% silt	St * M	2.49	36	110	***	
% N	St * M	3.58	36	110	***	√
% C	St * M	4.02	36	110	***	
Permeability	St * M	3.05	36	110	***	
SCOC	St * M	2.64	36	110	***	
NH _x	St * M	4.40	36	110	***	
NO _x	St * M	5.09	36	110	***	
TA	St * M	1.77	36	110	*	
DIC	St	45.52	2	9	***	
Nitrification	St * M	5.16	36	110	***	
Denitrification	St * M	4.88	36	110	***	
Max. oxygen penetration depth = max. depth where oxygen is present	St * M	10.82	29	81	***	
Macrobenthic density	St	38.50	9	110	***	√
Macrobenthic species richness	St	35.13	9	110	***	
	M	4.35	9	110	***	
Macrobenthic biomass	St	24.78	9	110	***	√
Bioturbation potential	St	36.42	9	110	***	√

Single factor results are only given where the interaction station * month (St * M) is not significant. Significance levels are indicated with * (0.01 < *P* < 0.05), ** (0.001 < *P* < 0.01), or *** (*P* < 0.001).

autocorrelation between sampling events was investigated by plotting the autocorrelation factor (ACF) versus the time lag. In case these plots indicated temporal autocorrelation, we re-ran the model with an auto-regressive model of order 1 (AR-1) autocorrelation structure, specifying the “corAR1” correlation option with respect to sampling event. We compared the models with and without autocorrelation structure using Akaike’s information criterion (AIC). Once the appropriate random component had been determined, the fixed component of the model was refined by manual backwards stepwise selection using ML to remove insignificant variable terms. The minimal adequate model was presented using REML (West and Welch 2006). Following Underwood (1997), the highest order significant interactions in the minimal adequate model were examined, but the nested levels within these were not. The importance of the highest order term was estimated using a likelihood ratio (*L* ratio) test to compare the full minimal adequate model with a model in which the relevant variable and all the interaction term that it was involved in, was omitted. Fluxes were expressed as a function of the independent environmental variables and macrobenthic descriptors. Only cases with information on

all variables (*n* = 165) were used in the models. Models with different combinations of variables and their centered (to reduce collinearity) quadratic terms were evaluated. Adding a temporal autocorrelation component to the models of SCOC and NH_x decreased the temporal pattern in the residuals and lowered the AIC. The importance of faunal predictor’s density and BPC was assessed by comparing nested models with and without faunal predictors, using ML (*L* ratio) tests. In addition, models including BPC as predictor were evaluated for muddy, fine-grained, and permeable sediment types separately. All analyses were performed in the free statistical environment R, except for the multivariate analyses carried out in Primer v6 (Clarke and Gorley 2006). Unless indicated differently, results are expressed as mean ± standard deviation.

RESULTS

Spatial and Temporal Variability in Benthic–Pelagic Coupling

Chl-*a* concentrations in the water column of the Southern North Sea followed clear temporal and

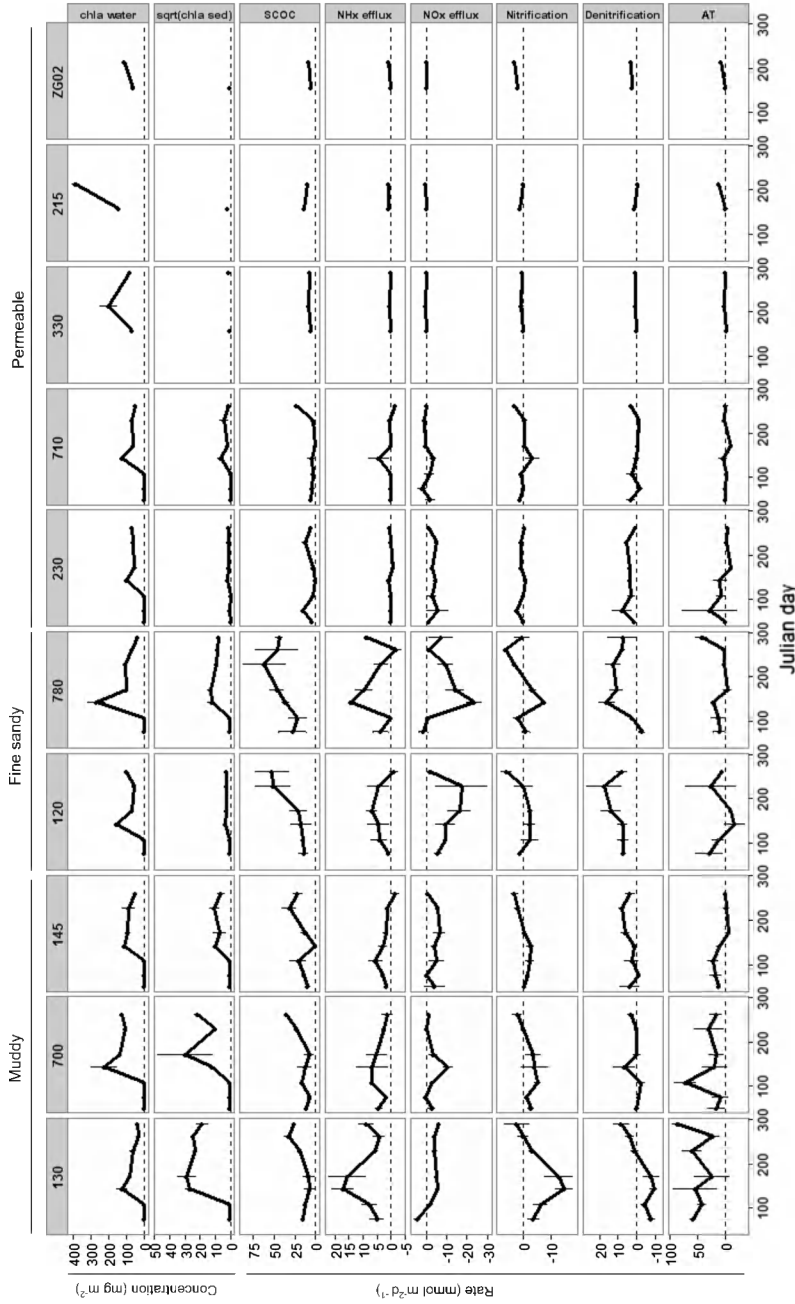


Figure 2. Chlorophyll-*a* in overlying water (1 m above the sea floor, integrated over water depth) and in the surface sediment (upper 2 cm; sqrt transformed for better visualization), measured SCOC ($\text{mmol O}_2 \text{ m}^{-2} \text{ d}^{-1}$), NH_x effluxes, potential NO_x effluxes ($\text{mmol N m}^{-2} \text{ d}^{-1}$), estimated nitrification and denitrification ($\text{mmol N m}^{-2} \text{ d}^{-1}$), and measured alkalinity flux ($\text{meq m}^{-2} \text{ d}^{-1}$) in all stations over time (mean \pm SD). No data for St. 780, 120, and 130 in February. Note the different scales on y-axes.

spatial patterns (Figure 2; two-way ANOVA see Table 1). In the near-shore stations 120, 130, 145, 700, 230, 710 and the more offshore located station 780, concentrations were low from February to April ($0.02 \pm 0.02 \mu\text{g l}^{-1}$), followed by a clear peak in chl-*a* at the end of May ($12.18 \pm 4.07 \mu\text{g l}^{-1}$). After this spring bloom peak, chl-*a* concentrations declined sharply ($5.88 \pm 2.71 \mu\text{g l}^{-1}$). A certain portion of the peak bloom arrived at the sediment from May onward (Figure 2). In the offshore stations 215, 330, and ZG02, chl-*a* concentrations in the overlying water in August ($9.82 \pm 3.76 \mu\text{g l}^{-1}$) were double those in June ($3.94 \pm 1.08 \mu\text{g l}^{-1}$). Owing to strong benthic–pelagic coupling, a pattern of spatio-temporal differences in the water column pigments is also reflected in the chl-*a* concentrations in the sediment (two-way ANOVA, Table 1; Figure 2).

Sediment median grain size, silt content, % organic N, and permeability differed among stations and time (Table 1), but a Tukey HSD test indicated mostly differences among stations. Based on the Wentworth granulometry scale (Wentworth 1922) and calculated permeability (Appendix D in Electronic Supplementary Material), the sampled stations can be classified into “muddy” (St. 130, 145, and 700), “fine sandy” (St. 120, and 780), and “permeable” sediments (near-shore St. 230 and 710 and offshore St. 330, 215, and ZG02) and will be named as such henceforth.

Spatial and Temporal Variability in Biogeochemical Cycling and Macrobenthic Functional Biodiversity

All measured fluxes differed among stations and time (two-way ANOVA, Table 1), but again a Tukey HSD test indicated mostly differences among stations. Macrobenthic characteristics varied mainly among station (two-way ANOVA, Table 1) and separate macrobenthic communities could be distinguished. Two-way-crossed ANOSIM revealed differences in community composition between stations ($R = 0.582$, $P < 0.001$) and sampling months (0.207 , $P < 0.001$). Pairwise tests indicated that muddy St. 130, 700, and 145 and permeable St. 230 and 710 were similar ($P > 0.05$) in terms of macrobenthic community composition. The temporal effect consists of a shift in composition from spring to autumn. The SIMPER results that characterize each station by the most abundant species are shown in Appendix E in Electronic Supplementary Material.

Muddy Sediments

St. 130, 145, and 700 showed the maximum OM content (averages of the muddy stations ranged between 1.10–1.91 % of organic carbon and 0.12–0.30 % organic nitrogen, Appendix D in Electronic Supplementary Material) and a stable annual maximum oxygen penetration depth (“OPD,” that is, the maximum depth where oxygen is still present) ranging between $3.4 \pm 0.2 \text{ mm}$ (St. 130) and $3.7 \pm 0.2 \text{ mm}$ (St. 145 and 700). Despite the substantial OM content, these stations displayed only moderate SCOC rates (Figure 2). St. 145 had a variable SCOC ($0\text{--}41.92 \text{ mmol O}_2 \text{ m}^{-2} \text{ d}^{-1}$), with a minimum in May (Tukey HSD $P < 0.05$). SCOC at St. 130 and 700 showed a more regular pattern, with low values early in the year ($12.10 \pm 3.36 \text{ mmol O}_2 \text{ m}^{-2} \text{ d}^{-1}$), gradually increasing to maximum rates in September ($33.99 \pm 2.81 \text{ mmol O}_2 \text{ m}^{-2} \text{ d}^{-1}$). These elevated summer SCOC rates coincided with a high water column temperature ($16 \text{ }^\circ\text{C}$), and showed a time lag of 3–4 months with respect to the deposition of the phytoplankton bloom in May–June (Figure 2). In contrast, increased ammonium effluxes (average of St. 130 and 700 in May and June, respectively, 16.34 ± 5.00 and $5.94 \pm 4.44 \text{ mmol N-NH}_4 \text{ m}^{-2} \text{ d}^{-1}$) did immediately follow the phytoplankton bloom deposition, suggesting an offset in the timing of OM mineralization and O_2 consumption. These high mineralization rates also appear associated with a sharp decline in pH of up to 1 pH unit in the subsurface sediment layers (Figure 3). No pronounced nitrate exchange was observed, except for a nitrate efflux in March at St. 130 ($4.48 \pm 1.45 \text{ mmol N-NO}_x \text{ m}^{-2} \text{ d}^{-1}$) and the very variable nitrate effluxes in April (range -1.73 to $+33.34 \text{ mmol N-NO}_x \text{ m}^{-2} \text{ d}^{-1}$) and August (range -0.31 to $+42.49 \text{ mmol N-NO}_x \text{ m}^{-2} \text{ d}^{-1}$) at St. 700. These two replicates with extremely high NO_x effluxes were considered outliers and are not further used in models and also not shown in Figure 2. The maximum alkalinity effluxes of all stations were measured at St. 130 and 700. At St. 130, alkalinity effluxes were higher later in the year (maximum in October: $86.88 \pm 8.75 \text{ meq A}_T \text{ m}^{-2} \text{ d}^{-1}$), associated with elevated DIC effluxes (St. 130: $66.49 \pm 18.14 \text{ mmol DIC m}^{-2} \text{ d}^{-1}$ in October), which seem indicative of carbonate dissolution. No significant denitrification was measured using $\text{N}_2\text{:Ar}$ technique at St. 130 in October, which is in accordance with the very low denitrification values deduced from our mass budget approach at this station. Nitrification estimates based on the mass budget approach resulted in (unphysical) negative values until late summer for all muddy stations (September: $2.05 \pm 2.68 \text{ mmol N m}^{-2} \text{ d}^{-1}$), whereas denitrification estimates were

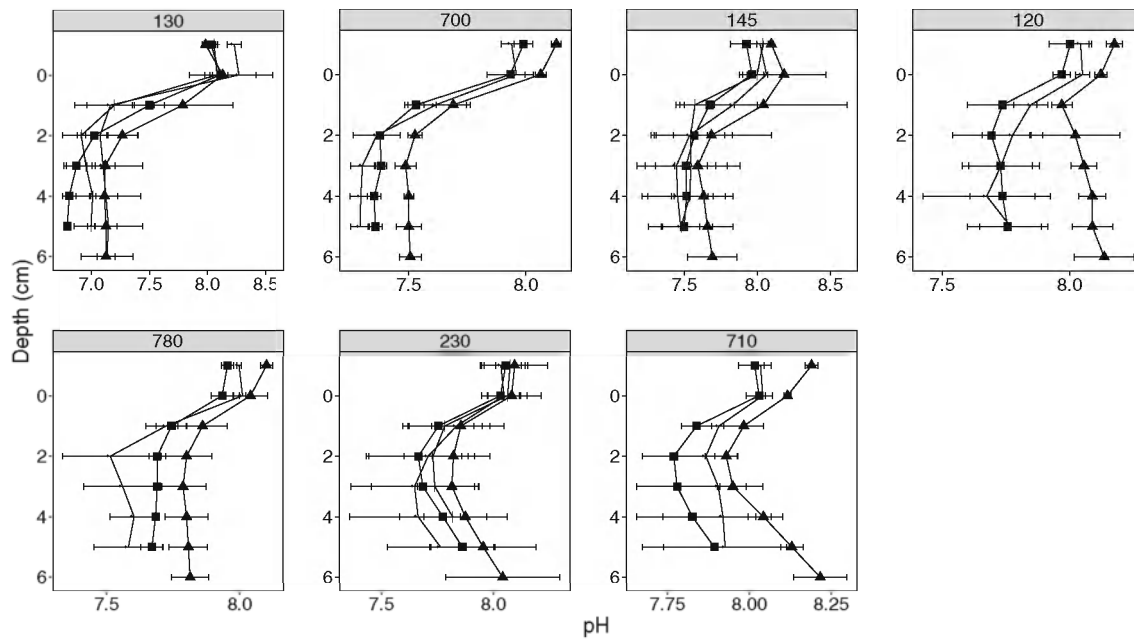


Figure 3. Sediment pH depth profiles (average \pm SD) in each station in February (filled triangle), March (filled circle), April (filled square), and May (plus). In May, only St. 130, 145, and 230 were profiled.

low but positive at St. 145 in all months but March, and positive from September on at St. 700 and 130 ($6.27 \pm 4.54 \text{ mmol N m}^{-2} \text{ d}^{-1}$) (Figure 2). Negative nitrification and denitrification estimates are not realistic. Rather, in these cases, the nitrification and denitrification processes are either zero or some of the assumptions underlying the mass budget were not justified (steady-state assumption; assumption that all reduced substances are reoxidized within the sediment). The latter explanation is corroborated by the low respiratory quotient (SCOC/DIC production) for St. 130 ($=0.39$), which implies that reduced compounds in the sediment are not efficiently reoxidized or that intensive carbonate dissolution occurs. Although the mass budget did not perform well in these muddy sediments, it highlights the need for data on sulfate reduction, the accumulation of reduced substances (for example, iron sulfides) and the dissolution of carbonate to effectively predict nitrogen cycling rates. This was beyond the scope of this study, but is crucial as guidance to future studies.

The muddy stations harbored little fauna, hence a low macrobenthic density ($527 \pm 795 \text{ ind. m}^{-2}$), biomass ($48.72 \pm 66.64 \text{ g WW m}^{-2}$), and species richness ($1.67 \pm 1.38 \text{ species core}^{-1}$). The fauna that is present, is characteristic of the *Macoma balthica* community (Degraer and others 2009) (see SIMPER results in Appendix E in Electronic Supplementary Material). The muddy sediments harbor mainly surficial modifiers (*Macoma balthica*

and small polychaetes, Appendices E and F in Electronic Supplementary Material) that in addition to their low densities and biomass in these sediments, have a limited influence on sediment reworking. This is reflected in a low BPC ($416.13 \pm 494.21 \text{ m}^{-2}$) (Figure 4).

Fine Sandy Sediments

St. 780 and 120 displayed an intermediate organic carbon (respectively, 0.40 and 0.52 %) and nitrogen (0.04–0.07 %) content (Appendix D in Electronic Supplementary Material) and an annual average maximum OPD of 3.9 ± 0.2 and $3.7 \pm 0.2 \text{ mm}$, respectively. This relatively shallow OPD corroborates the maximum oxygen consumption rates (average in August: $56.31 \pm 22.12 \text{ mmol O}_2 \text{ m}^{-2} \text{ d}^{-1}$), which coincides with the highest annual sea water temperature ($18 \text{ }^\circ\text{C}$), which is also a time lag of 3 months with respect to phytoplankton deposition (Figure 2). Moderate to high ammonium effluxes ($4.45 \pm 4.87 \text{ mmol N-NH}_x \text{ m}^{-2} \text{ d}^{-1}$) and clear nitrate influxes ($8.67 \pm 8.42 \text{ mmol N-NO}_x \text{ m}^{-2} \text{ d}^{-1}$) characterized these stations (Figure 2). At St. 780, maximum NH_x effluxes ($14.37 \pm 0.51 \text{ mmol N-NH}_x \text{ m}^{-2} \text{ d}^{-1}$) and NO_x influxes ($23.49 \pm 3.74 \text{ mmol N-NO}_x \text{ m}^{-2} \text{ d}^{-1}$) coincided with deposition of the phytoplankton bloom (Figure 2). Moderate alkalinity fluxes ($10.70 \pm 21.20 \text{ meq A}_T \text{ m}^{-2} \text{ d}^{-1}$) typify these fine sandy stations (Figure 2). At both

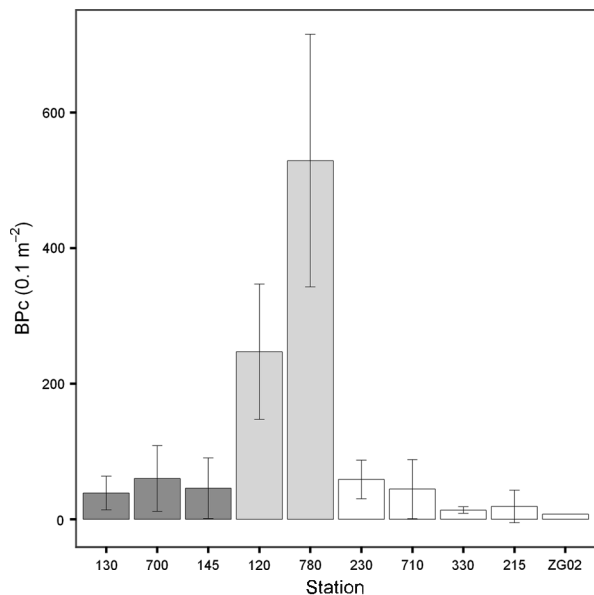


Figure 4. Bioturbation potential of the community (BPC) in each station averaged over the year (mean \pm SD). Muddy sediments are indicated in *dark gray bars*, fine sandy sediments in *light gray*, and permeable sediments in *white*.

stations, nitrification estimates in summer ($3.35 \pm 3.43 \text{ mmol N m}^{-2} \text{ d}^{-1}$) and denitrification estimates throughout the year ($11.01 \pm 8.16 \text{ mmol N m}^{-2} \text{ d}^{-1}$) were higher than at all other stations and a clear increase in modeled denitrification at the time of phytoplankton deposition was observed (Figure 2). Although the NO_x concentrations in the water column of the lab incubations were higher than those of the overlying water in the field, observed and modeled denitrification at St. 780 in October (measured: $5.54 \pm 1.02 \text{ mmol N m}^{-2} \text{ d}^{-1}$; modeled: $7.43 \pm 8.27 \text{ mmol N m}^{-2} \text{ d}^{-1}$) agreed reasonably well. This indicates that the mass budget model results are within realistic ranges for these stations. Sediment pH profiles showed an initial decline of about 0.25 pH units in the first 1–2 cm, after which they were stable in depth (Figure 3). The DIC efflux at St. 780 in October was comparable to the one measured at St. 130 ($62.70 \pm 13.24 \text{ mmol DIC m}^{-2} \text{ d}^{-1}$), but taking into account the increased SCOC ($43.88 \pm 4.84 \text{ mmol O}_2 \text{ m}^{-2} \text{ d}^{-1}$), this results in a more elevated respiratory quotient ($=0.70$) at this fine sandy station, which implies that reduced compounds in the sediment are more efficiently reoxidized, and/or that carbonate dissolution is less important.

St. 780 and 120 displayed macrobenthic abundances ($4,608 \pm 3,527 \text{ ind. m}^{-2}$), biomass ($411.69 \pm 488.32 \text{ g WW m}^{-2}$), and BPC ($3,952.89 \pm 2,813.37 \text{ m}^{-2}$)

(Figure 4) that are an order of magnitude higher than the muddy and permeable sediments (Tukey HSD $P < 0.05$). Maximum values of species richness ($7.44 \pm 2.74 \text{ species core}^{-1}$) were displayed in this sediment type (Tukey HSD $P < 0.05$). The fauna present belongs to the species rich and abundant *Abra alba* community (Van Hoey and others 2004) (see SIMPER results in Appendix E in Electronic Supplementary Material). The very high BPC in the fine sandy stations is mainly made up by the BPC of the biodiffusers *Echinocardium cordatum*, *Sagartia troglodytes*, and *Abra alba* (Appendix F in Electronic Supplementary Material). The total proportion of biodiffusers in the community is not that different from the biodiffuser proportion in other stations, but the biomass is the highest of all stations. At St. 780, also increased densities and biomass of surficial modifiers (mainly *Owenia fusiformis*) contribute to a higher BPC (Appendices E and F in Electronic Supplementary Material).

Permeable Sediments

Near-shore St. 230, 710 and offshore St. 215, 330, and ZG02 displayed the lowest organic carbon (averages of the permeable stations ranged between 0.10 and 0.25 %) and nitrogen content (0.02–0.09 %; Appendix D in Electronic Supplementary Material) and deeper oxygen penetration (annual average maximum OPD, respectively, 4.6 ± 0.4 and $7.8 \pm 1.2 \text{ mm}$ at St. 230 and 710), which correspond to a lower oxygen demand ($6.73 \pm 5.54 \text{ mmol O}_2 \text{ m}^{-2} \text{ d}^{-1}$), lower DIN exchange (average NH_x efflux of $0.44 \pm 1.26 \text{ mmol N-NH}_x \text{ m}^{-2} \text{ d}^{-1}$ and an average NO_x influx of $1.00 \pm 2.41 \text{ mmol N-NO}_x \text{ m}^{-2} \text{ d}^{-1}$) and lower alkalinity effluxes ($2.58 \pm 12.24 \text{ meq A}_T \text{ m}^{-2} \text{ d}^{-1}$) (Figure 2). The maximum OPD at St. 710 decreased with higher temperatures to $2.58 \pm 0.58 \text{ mm}$ (Tukey HSD $P < 0.05$); this increased diffusive oxygen uptake coincided with higher SCOC in September ($22.94 \pm 1.87 \text{ mmol O}_2 \text{ m}^{-2} \text{ d}^{-1}$). Denitrification was only observed in October in one core at St. 330 (measured: $1.80 \text{ mmol N m}^{-2} \text{ d}^{-1}$ vs. modeled: $0.62 \pm 0.05 \text{ mmol N m}^{-2} \text{ d}^{-1}$). Low SCOC ($6.63 \pm 2.18 \text{ mmol O}_2 \text{ m}^{-2} \text{ d}^{-1}$) was associated with an equally low DIC efflux ($6.95 \pm 2.41 \text{ mmol DIC m}^{-2} \text{ d}^{-1}$ at St. 330) in October, resulting in a respiratory quotient of 0.97. This implies little mineralization and a reoxidation of reduced mineralization products. Very low nitrification ($0.68 \pm 1.55 \text{ mmol N m}^{-2} \text{ d}^{-1}$) and denitrification ($2.13 \pm 3.39 \text{ mmol N m}^{-2} \text{ d}^{-1}$) rates were estimated throughout the year (Figure 2). Beyond an initial

decrease of about 0.25 U in sediment pH in the first centimeter, the pH stabilized, or even increased again at depth (St. 230 and 710 in all months) (Figure 3).

The fauna present in these permeable sediments belongs to the species-poor *Nephtys cirrosa* and *Ophelia limacina* communities (Van Hoey and others 2004) (see SIMPER results in Appendix E in Electronic Supplementary Material). Macrobenthic density (548 ± 775 ind. m^{-2}), biomass (17.33 ± 40.14 g WW m^{-2}), species richness (2.28 ± 2.00 species core $^{-1}$), and BPC (303.34 ± 376.90 m^{-2}) in these stations are low, but comparable to the very muddy stations (Figure 4). However, other than surficial modifiers (bivalves such as *Ensis directus*), there were also biodiffusers (small *Echinocardium cordatum* and *Glycera alba*) and upward (downward) conveyors present (different Capitellidae and Spionidae species), that nevertheless contributed little to BPC because of low biomass and density (Appendices E and F in Electronic Supplementary Material)

Statistical Modeling of Fluxes from Abiotic and Biotic Environmental Variables

The statistical models that best predicted SCOC, NH_x , alkalinity efflux, and denitrification included strong effects of BPC and were significantly better performing (that is, had a lower AIC and *L* ratio) than similar models with macrobenthic density as the faunal component (Table 2). The best model predicting denitrification included only a strong effect of BPC and its quadratic term (Denitrification 2, Table 2). The best model predicting nitrification was the only model that included medium effects of both BPC and density. Median grain size was further an important explanatory variable for all modeled processes but denitrification. Temperature was significantly contributing to the explained variance in SCOC and nitrification and to a lesser extent also NH_x and alkalinity efflux, whereas chl-*a* in the water column was only important for NH_x and alkalinity effluxes.

When fluxes were modeled per sediment type, BPC appeared as an important explanatory variable in predicting fluxes in fine sandy sediments (SCOC, NH_x , denitrification, and alkalinity model, Appendix G in Electronic Supplementary Material) and to a lesser extent in permeable sediments (SCOC, nitrification, and denitrification model). In contrast, BPC was never significantly contributing to explaining fluxes in muddy sediments; macrobenthic density appeared more important in this case (NH_x , nitrification, and alkalinity model).

DISCUSSION

The Southern North Sea harbors a variety of benthic habitat types, both in terms of sedimentology (Verfaillie and others 2006) and macrobenthic biodiversity (Van Hoey and others 2004; Degraer and others 2008). This study also showed that biogeochemical cycling clearly differs among habitat types and throughout the year. The annual spring phytoplankton bloom, deposited on the sea floor in May, results in a substantial input of OM to the benthic ecosystem. The observed patterns in chl-*a* in sediment and overlying water are consistent with the phytoplankton dynamics previously described for the Southern Bight of the North Sea (for example, Lancelot and others 2005; Rousseau and others 2002). Benthic–pelagic coupling was strong at most stations: the peak in sediment chl-*a* coincided with the peak in the overlying water and the deposition event triggered OM mineralization processes at the sea floor, which differed according to sediment type.

Whereas the deposition of the phytoplankton bloom in spring to muddy sediments was immediately evidenced by high ammonium effluxes, the highest oxygen consumption was delayed until summer when temperatures reached a maximum. The deposition event has been shown to trigger the microbial loop in the muddy sediments of the Southern North Sea (Pede 2012), which can indeed initiate the first degradation of particulate OM to ammonium (Jensen and others 1990; Grenz and others 2000). However, in other shallow coastal seas as well, the time lag in oxygen consumption has been demonstrated (Kannevorff and Christensen 1986; Rudnick 1989), revealing the temperature dependency of sedimentary biogeochemical processes (Provoost and others 2013). Because of the increased OM content and bacterial abundances (Gillan and others 2012), the cohesion of the sediment matrix and the lack of bioturbating fauna in the muddy stations, oxygen rapidly becomes depleted in the upper millimeters. The small amount of oxygen present in these muddy sediments is probably mostly used for oxic mineralization and sulfide re-oxidation, because the estimated nitrification rates are low throughout most of the year. In addition, estimated and measured denitrification rates were small to non-detectable. At sites with elevated OM mineralization rates, denitrification is often reduced through sulfide inhibition of nitrifying bacteria or by inhibition of coupled nitrification–denitrification in oxygen-deficient sediment (Joye and Hollibaugh 1995; Eyre and Ferguson 2002). In this case, most of the nitrogen returns to the water

Table 2. Oxygen Consumption (SCOC), Ammonium (NH_x) and Alkalinity (A_T) Effluxes and Nitrification and Denitrification Estimates as a Function of Environmental Variables Temperature (Temp), Median Grain Size (MGS), Chlorophyll-*a* Concentration in the Water Column (chl-*a*), Macrobenthic Density (Dens) and Bioturbation Potential of the Community (BPC), and Their Centered Quadratic Terms

Model	Model formula	AIC	L ratio fauna term
SCOC1	$SCOC = 2.35 + 0.003 Dens^{***} - 0.034 MGS^{***} + 6.93e^{-05} MGS^{2***} + 0.787 Temp^{***} + 0.086 Temp^{2*}$	1,254.063	17.35
SCOC2	$SCOC = 0.75 + 0.005 BPC^{***} - 0.033 MGS^{***} + 7.38e^{-05} MGS^{2***} + 0.839 Temp^{***} + 0.092 Temp^{2**}$	1,221.676	49.94
NH _x 1	$NH_x = 2.15^{***} + 2.1e^{-04} Dens^{***} - 0.01 MGS^{***} + 3.6e^{-05} MGS^{2***} + 0.04 Temp + 0.01 Temp^{2*} + 0.09 chl-a^{**}$	785.5602	2.67
NH _x 2	$NH_x = 1.75^{**} + 6.37e^{-04} BPC^{***} - 0.01 MGS^{***} + 3.1e^{-05} MGS^{2***} + 0.07 Temp^{*} + 0.01 Temp^{2*} + 0.09 chl-a^{***}$	771.6502	16.58
Nitrification1	$Nitrification = -5.69^{***} - 5e^{-04} Dens^{**} + 6.03e^{-08} Dens^{2*} + 9.5e^{-04} BPC^{**} - 1.5e^{-07} BPC^{2**} + 0.006 MGS^{***} - 3.4e^{-05} MGS^{2**} + 0.36 Temp^{***} + 0.05 Temp^{2***} - 0.21 chl-a^{***}$	920.3118	Density: 7.95 BPC: 9.71
Denitrification1	$Denitrification = 0.59^{**} + 0.002 Dens^{***} - 2.00e^{-07} Dens^{2**}$	1,050.058	Dens + Dens ² : 41.14
Denitrification2	$Denitrification = 0.68^{***} + 0.004 BPC^{***} - 3.00e^{-07} BPC^{2***}$	1,035.271	BPC + BPC ² : 54.49
Alkalinity1	$Alkalinity = -8.94 + 0.002 Dens^{***} - 0.04 MGS^{***} + 2.0e^{-04} MGS^{2***} + 1.18 Temp^{*} + 0.16 Temp^{2*} - 0.83 chl-a + 0.16 chl-a^{2**}$	1,415.762	10.83
Alkalinity2	$Alkalinity = -8.93 + 0.002 BPC^{***} - 0.04 MGS^{***} + 2.0e^{-04} MGS^{2***} + 1.16 Temp^{*} + 0.15 Temp^{2*} - 0.81 chl-a + 0.17 chl-a^{2**}$	1,413.818	12.41

Significance of terms (* $P < 0.05$, ** $P < 0.01$, *** $P < 0.001$) and the AIC as determined with restricted maximum likelihood of the best models are given; bold AIC values indicate the best model.

column as NH_4^+ , especially after the phytoplankton bloom deposition, which creates a positive feedback to eutrophication in an area that is already sensitive to oxygen stress (Van Hoey and others 2009). Alternatively, nitrate can be turned into NH_x through dissimilatory nitrate reduction to ammonium (DNRA) (Hulth and others 2005), again stimulating a release of NH_4^+ to the water column.

The muddy sediments displayed the highest alkalinity effluxes of all sampled stations, with a maximum in summer at St. 130. This corroborates the earlier observed seasonal variability in sediment–water alkalinity fluxes in the North Sea (Thomas and others 2009). Important sources of alkalinity generation in coastal areas include sulfate reduction with the formation of metal sulfides and to a lesser extent denitrification (Chen and Wang 1999; Thomas and others 2009). Because denitrification estimates were low at the muddy stations, it is probably either sulfate reduction (and the subsequent accumulation of pyrite) or the dissolution of carbonate that generates the high alkalinity effluxes at this station. Increased sulfide accumulation at depth has been observed at St. 130 (Malkin and others, accepted; Gao and others 2009), which indicates that intensive sulfate reduction is indeed taking place. However, electrogenic filamentous bacteria have recently been discovered at St. 130 (Malkin and others, accepted). Although Hu and Cai (2011) argue that only net sulfate reduction (with the formation of metal sulfides) contributes to alkalinity generation in sediments, this novel electrogenic pathway of sulfide oxidation may generate high alkalinity effluxes. Electrogenic sulfur oxidation strongly consumes protons within the upper layer of the sediment (Nielsen and others 2010), and this way, it creates a zone of high alkalinity generation in the upper millimeters of the sediment, potentially driving the observed efflux of alkalinity out of the sediment. In addition, electrogenic sulfur oxidation has been associated with strong carbonate dissolution at depth (Risgaard-Petersen and others 2012), thus providing a second pathway for sedimentary alkalinity generation.

The response to phytoplankton bloom deposition in the fine sandy sediments in terms of ammonium effluxes and oxygen consumption was very similar to the one described for muddy sediments. Although the OM content of these fine sandy sediments is substantial, the abundant bioturbating and bio-irrigating fauna keep the sediment sufficiently oxygenated to stimulate nitrification. The produced nitrate can then serve as a substrate for denitrification. The importance of bioturbation and bio-irrigation processes has been shown to enhance

coupled nitrification–denitrification (Pelegri and others 1994; Rysgaard and others 1995). Maximum estimates of both nitrification (in summer) and denitrification (throughout the year) were indeed found at the fine sandy stations, which suggest intensified coupled nitrification–denitrification (Cornwell and others 1999). Denitrification is an important process, because it effectively removes fixed nitrogen from the system (Seitzinger 1988). However, increased denitrification would lead to higher alkalinity fluxes, which is not supported by our observations. The lower alkalinity effluxes at St. 780 and 120 can probably be attributed to enhanced reoxidation of reduced substances by irrigating fauna, and/or reduced rates of carbonate dissolution. The same accounts for the temporal trend in alkalinity fluxes: because of oxygen deficiency, it is supposed that more anaerobic processes take place in summer, but because fauna are also more active at this time (Maire and others 2007; Braeckman and others 2010), enhanced reoxidation of the reduced substances takes place (Eyre and Ferguson 2002). These observations clearly confirm the importance of bioturbating and bio-irrigating fauna for benthic carbon and nitrogen mineralization.

Overall, very small benthic fluxes were observed in the permeable sediments. Because of the efficient reoxidation of reduced substances, alkalinity effluxes are also very low. The near-shore St. 230 and 710 evidenced more pronounced fluxes than the offshore permeable stations, although the latter were subjected to an experimentally induced advective current into the sediment. However, because SCOC observed at St. 330 is similarly low as the measurements without the centrally stirring disk in Franco and others (2010) at the same station, the advective flow here applied was probably too weak to really simulate the hydrodynamic forces experienced in the field. On the other hand, there might be no OM left in these permeable sediments because they recycle fresh OM quickly (Huettel and others 2003; Rasheed and others 2003). Taking into account the substantial inflow of oxygenated sea water into permeable sediments under in situ conditions, it is possible that these sediments are equally if not even more important than muddy and fine sandy sediments in terms of carbon mineralization (Gao and others 2012), especially when OM is deposited on the sea floor (Huettel and others 2003; Rasheed and others 2003). Non-invasive in situ measurements such as the Eddy correlation technique (Berg and others 2003) should be compared to core incubations in the near future.

For the development of the statistical models predicting measured or estimated processes, not all the measured environmental variables were included. Preliminary models also showed the importance of sediment chl-*a* and organic nitrogen content of the sediment. However, to facilitate future spatial extrapolation of the measured biogeochemical cycling processes, we chose to use only those environmental parameters for which full coverage maps exist [sediment median grain size (Verfaillie and others 2006), temperature and chl-*a* in the water column (MODIS and MERIS satellite data, <http://www2.mumm.ac.be/remsem/index.php>)], or will be available in the near future (macrobenthic density and BPC).

Several studies have estimated fluxes from environmental variables, extrapolating from, for example, sediment porosity, chl-*a* content and bottom water nutrient concentration (Grenz and others 2000), sediment permeability (Gao and others 2012), granulometry, sediment oxygen content and organic carbon content (Deutsch and others 2010), depth and primary production (Wenzhöfer and Glud 2002), and nitrate availability in the overlying water and granulometry (Deek and others 2012). None of these studies take into account biotic parameters. Effects of biodiversity can be hard to detect in natural systems, because variability of environmental variables outweighs the mediating effects of biota (Raffaelli 2006; Godbold and Solan 2009). For our study area however, significantly better statistical models were obtained when including biotic information: in all models, BPC or macrobenthic density was essential in explaining spatio-temporal variability in fluxes. The importance of BPC for biogeochemical processes depended also on sediment type: BPC was a crucial predictor variable for SCOC, NH_x efflux, and alkalinity efflux and denitrification in fine sandy sediments and to a lesser extent for permeable sediments, whereas fluxes in muddy sediments depended on abiotic variables and/or macrobenthic density. This makes clear that the importance of functional biodiversity for carbon cycling is not equal across all habitat types.

The unequal importance of BPC across habitats can be explained by the inherent biotic and abiotic characteristics of each habitat: macrobenthic abundance and biomass, hence also BPC is typically low in cohesive and permeable sediments. If any macrofauna at all are present in the oxygen-depleted muddy sediments, they have to stay in contact with the oxygen-rich overlying water, either by dwelling at the surface (surficial modifiers that have limited impact on sediment reworking) or by using siphons or by ventilation of their bur-

rows, hence bio-irrigation, a mechanism that is not accounted for in BPC. In permeable sediments, advective pore water transport overrules the effect of bioturbating fauna (Kristensen and Kostka 2005). In the fine sandy sediments, macrofauna densities and biomass are highest, but still, the elevated BPC values are mainly made up by bio-diffusers: a few but large sea urchins (*Echinocardium cordatum*) and many but small bivalves (*Abra alba*). Where present, dense aggregations of surface-modifying tube worms (*Owenia fusiformis*) can also contribute to nearly half of the BPC. So in areas where functional diversity is important, it stands out compared to species richness, density, or biomass alone.

Although the goodness-of-fit was higher when models included BPC compared to models with only abiotic variables, we have to keep in mind that BPC has some other drawbacks. The bioturbation potential of a species is assumed to be context independent; the activity of an organism is independent of the ruling environmental conditions such as temperature and disturbance (Queirós and others 2013). In addition, BPC is a summation of single species effects, biomass, and abundance (Solan and others 2004), whereas many laboratory experiments with artificial communities have shown that the effect of multispecies assemblages on biogeochemical processes are not per se the summation of the single species effects (Waldbusser and others 2004; Mermillod-Blondin and others 2005; Godbold and others 2008). This again shows that our understanding of how fauna and environment interact with each other while influencing OM cycling is still limited (Teal and others 2013). In summary, there is room for improving the proxy for functional biodiversity (BPC), by including measures of interaction between species and their biotic and abiotic environment and by introducing a measure for bio-irrigation.

Notwithstanding its above-mentioned drawbacks, the BPC metric encompassing density, biomass, and functional trait parameters such as bioturbation fashion and intensity appears to explain the variability in fluxes much better than macrobenthic density or biomass alone (this study, Van Colen and others 2012). Especially for monitoring of marine habitats in the framework of the European Marine Strategy, this functional biodiversity index proves valuable for establishing a comprehensive link with carbon mineralization (Birchenough and others 2012; Queirós and others 2013), mainly for fine sandy sediments. Here, a loss of macrobenthic functional diversity might bring along a loss in OM cycling. Because changes in

biota can have greater effects on ecosystem properties than changes in abiotic conditions (Hooper and others 2005), it is crucial to maintain this macrobenthic functional diversity.

CONCLUSIONS

This study shows that a wide diversity in habitat types exists in the Southern North Sea, not only in terms of macrobenthic functional biodiversity, but also in terms of biogeochemical cycling. The muddy sediments in our study area appear especially important in alkalinity generation. Biogeochemical cycling in the fine sandy sediments was strongly influenced by macrobenthic functional biodiversity, where BPc was shown to be an important metric in explaining SCOC, denitrification, alkalinity fluxes, and NH_x fluxes. Our results pinpoint the strong link between macrobenthic functional biodiversity and carbon and nitrogen mineralization, especially in fine sandy sediments. This has the important implication that a loss of macrobenthic functional diversity entails a loss in benthic ecosystem functioning.

ACKNOWLEDGMENTS

We are very grateful to the two anonymous reviewers who considerably helped us to improve this manuscript. We are further indebted to the crew of R.V. Zeeleeuw for help with sampling at sea, to Yves Israël for the development of the experimental set-up, to Sofie Jacob, Bart Beuse-linck, Niels Viaene, Liesbet Colson, Hannah Marchant, Dr. Gaute Lavik, and Jurian Brassier for help with sample processing and to Heiko Brenner, Sairah Malkin, Alexandra Rao, and attendants of the Wadden Sea Processes Mini-Workshop at Hamburg University for fruitful discussions. Kristof Van Steelandt from FIRE Statistical Consulting is acknowledged for statistical support. U.B. was financially supported by FWO Project No. G.0033.11. Additional funding was provided by the Special Research Fund of Ghent University (BOF-GOA 01GA1911W).

REFERENCES

Aller R. 1988. Benthic fauna and biogeochemical processes in marine sediments: the role of burrow structures. In: Blackburn TH, Sørensen J, Eds. Nitrogen cycling in coastal marine environments. SCOPE, Vol. 33. Chichester: Wiley, Ltd. p 301–38.

Benton TG, Solan M, Travis JMJ, Sait SM. 2007. Microcosm experiments can inform global ecological problems. *Trends Ecol Evol* 22:516–21.

Berg P, Røy H, Janssen F, Meyer V, Jørgensen B, Huettel M, de Beer D. 2003. Oxygen uptake by aquatic sediments measured with a novel non-invasive eddy-correlation technique. *Mar Ecol Prog Ser* 261:75–83.

Birchenough SNR, Parker RE, McManus E, Barry J. 2012. Combining bioturbation and redox metrics: potential tools for assessing seabed function. *Ecol Indic* 12:8–16.

Blackburn TH. 1988. Benthic mineralization and bacterial production. In: Blackburn TH, Sørensen J, Eds. Nitrogen cycling in coastal marine environments. SCOPE, Vol. 33. Chichester: Wiley, Ltd. p 175–90.

Braeckman U, Provoost P, Gribsholt B, Van Gansbeke D, Middelburg JJ, Soetaert K, Vincx M, Vanaverbeke J. 2010. Role of macrofauna functional traits and density in biogeochemical fluxes and bioturbation. *Mar Ecol Prog Ser* 399:173–86.

Bulling MT, Hicks N, Murray L, Paterson DM, Raffaelli D, White PC, Solan M. 2010. Marine biodiversity–ecosystem functions under uncertain environmental futures. *Philos Trans R Soc B Biol Sci* 365:2107.

Cardinale BJ, Duffy JE, Gonzalez A, Hooper DU, Perrings C, Venail P, Narwani A, Mace GM, Tilman D, Wardle DA. 2012. Biodiversity loss and its impact on humanity. *Nature* 486:59–67.

Chen CTA. 2002. Shelf- vs. dissolution-generated alkalinity above the chemical lysocline. *Deep Sea Res II* 49:5365–75.

Chen CTA, Wang SL. 1999. Carbon, alkalinity and nutrient budgets on the East China Sea continental shelf. *J Geophys Res* 104:20675–86.

Clarke KR, Gorley RN. 2006. Primer v6: user manual/tutorial. Plymouth: PRIMER-E.

Cornwell JC, Kemp WM, Kana TM. 1999. Denitrification in coastal ecosystems: methods, environmental controls, and ecosystem level controls, a review. *Aquat Ecol* 33:41–54.

Deek A, Emeis K, van Beusekom J. 2012. Nitrogen removal in coastal sediments of the German Wadden Sea. *Biogeochemistry* 108:1–17.

Degraer S, Verfaillie E, Willems W, Adriaens E, Vincx M, Van Lancker V. 2008. Habitat suitability modelling as a mapping tool for macrobenthic communities: an example from the Belgian part of the North Sea. *Cont Shelf Res* 28:369–79.

Degraer S, Braeckman U, Haelters J, Hostens K, Jacques TG, Kerckhof F, Merckx B, Rabaut M, Stienen EWM, Van Hoey G, et al. 2009. Studie betreffende het opstellen van een lijst met potentiële Habitatrichtlijngebieden in het Belgische deel van de Noordzee. Eindrapport, 93 pp.

Deutsch B, Forster S, Wilhelm M, Dippner JW, Voss M. 2010. Denitrification in sediments as a major nitrogen sink in the Baltic Sea: an extrapolation using sediment characteristics. *Biogeosciences* 7:3259–71.

Doney SC. 2010. The growing human footprint on coastal and open-ocean biogeochemistry. *Science* 328:1512–16.

Eggleston J, Rojstaczer S. 1998. Inferring spatial correlation of hydraulic conductivity from sediment cores and outcrops. *Geophys Res Lett* 25:2321–4.

Emmerson MC, Raffaelli DG. 2000. Detecting the effects of diversity on measures of ecosystem function: experimental design, null models and empirical observations. *Oikos* 91:195–203.

Eyre BD, Ferguson AJ. 2002. Comparison of carbon production and decomposition, benthic nutrient fluxes and denitrification in seagrass, phytoplankton, benthic microalgae- and macro-

U. Braeckman and others

- algae-dominated warm-temperate Australian lagoons. *Mar Ecol Prog Ser* 229:43–59.
- Forster S, Bobertz B, Bohling B. 2003. Permeability of sands in the coastal areas of the southern Baltic Sea: mapping a grain-size related sediment property. *Aquat Geochem* 9:171–90.
- Franco M, Vanaverbeke J, Van Oevelen D, Soetaert K, Costa MJ, Vincx M, Moens T. 2010. Respiration partitioning in contrasting subtidal sediments: seasonality and response to a spring phytoplankton deposition. *Mar Ecol* 31:276–90.
- Gao Y, Lesven L, Gillan D, Sabbe K, Billon G, De Galan S, Elskens M, Baeyens W, Leermakers M. 2009. Geochemical behavior of trace elements in sub-tidal marine sediments of the Belgian coast. *Mar Chem* 117:88–96.
- Gao H, Matyka M, Liu B, Khalili A, Kostka JE, Collins G, Jansen S, Holtappels M, Jensen MM, Badewien TH et al. 2012. Intensive and extensive nitrogen loss from intertidal permeable sediments of the Wadden Sea. *Limnol Ocean* 57:185.
- Gérino M, Stora G, Francois F, Gilbert F, Poggiale JC, Mermillod-Blondin F, Desrosiers G, Vervier P. 2003. Macro-invertebrate functional groups in freshwater and marine sediments: a common mechanistic classification. *Vie Milieu* 53:221–32.
- Gilbertson WW, Solan M, Prosser JJ. 2012. Differential effects of microorganism–invertebrate interactions on benthic nitrogen cycling. *FEMS Microbiol Ecol* 82:11–22.
- Gillan DC, Pede A, Sabbe K, Gao Y, Leermakers M, Baeyens W, Loureiro Cabana B, Billon G. 2012. Effect of bacterial mineralization of phytoplankton-derived phytodetritus on the release of arsenic, cobalt and manganese from muddy sediments in the Southern North Sea. A microcosm study. *Sci Total Environ* 419(2012):98–108.
- Godbold J, Solan M. 2009. Relative importance of biodiversity and the abiotic environment in mediating an ecosystem process. *Mar Ecol Prog Ser* 396:273–82.
- Godbold JA, Solan M, Killham K. 2008. Consumer and resource diversity effects on marine macroalgal decomposition. *Oikos* 118:77–86.
- Grenz C, Cloern JE, Hager SW, Cole BE. 2000. Dynamics of nutrient cycling and related benthic nutrient and oxygen fluxes during a spring phytoplankton bloom in South San Francisco Bay (USA). *Mar Ecol Prog Ser* 197:67–80.
- Halpern BS, Walbridge S, Selkoe KA, Kappel CV, Micheli F, D'Agrosa C, Bruno JF, Casey KS, Ebert C, Fox HE, Fujita R, Heinemann D, Lenihan HS, Madin EMP, Perry MT, Selig ER, Spalding M, Steneck R, Watson R. 2008. A global map of human impact on marine ecosystems. *Science* 319:948–52.
- Heiberger RM, Holland B. 2004. Statistical analysis and data display: an intermediate course with examples in S-plus, R, and SAS. Springer.
- Hooper D, Chapin F, Ewel J, Hector A, Inchausti P, Lavorel S, Lawton J, Lodge D, Loreau M, Naeem S, Schmid B, Setälä H, Symstad A, Vandermeer J, Wardle D. 2005. Effects of biodiversity on ecosystem functioning: a consensus of current knowledge. *Ecol Monogr* 75:3–35.
- Hu X, Cai WJ. 2011. An assessment of ocean margin anaerobic processes on oceanic alkalinity budget. *Glob Biogeochem Cycles* 25:GB3003.
- Huetzel M, Rusch A. 2000. Transport and degradation of phytoplankton in permeable sediment. *Limnol. Oceanogr.* 45:534–49.
- Huetzel M, Roy H, Precht E, Ehrenhauss S. 2003. Hydrodynamical impact on biogeochemical processes in aquatic sediments. *Hydrobiologia* 494:231–6.
- Hulth S, Aller RC, Canfield DE, Dalsgaard T, Engstrom P, Gilbert F, Sundback K, Thamdrup B. 2005. Nitrogen removal in marine environments: recent findings and future research challenges. *Mar Chem* 94:125–45.
- Ineno EN, Solan M, Batty P, Pierce GJ. 2006. How biodiversity affects ecosystem functioning: roles of infaunal species richness, identity and density in the marine benthos. *Mar Ecol Prog Ser* 311:263–71.
- Jensen MH, Lomstein E, Sørensen J. 1990. Benthic NH₄ and NO₃ flux following sedimentation of a spring phytoplankton bloom in Aarhus Bight, Denmark. *Mar Ecol Prog Ser* 61:87–96.
- Jørgensen BB. 1983. Processes at the sediment–water interface. In: Bolin B, Cook RB, Eds. *Major biogeochemical cycles their interactions*. New York: Wiley. p 477–515.
- Joye SB, Hollibaugh JT. 1995. Influence of sulfide inhibition of nitrification on nitrogen regeneration in sediments. *Science* 270:623–5.
- Kana T, Darkangelo C, Hunt M, Oldham J, Bennett G, Cornwell J. 1994. Membrane inlet mass-spectrometer for rapid high-precision determination of N₂, O₂ and in Ar in environmental water samples. *Anal Chem* 66:4166–70.
- Kanneworff E, Christensen H. 1986. Benthic community respiration in relation to sedimentation of phytoplankton in the Øresund. *Ophelia* 26:269–84.
- Kristensen E, Kostka JE. 2005. Macrofaunal burrows and irrigation in marine sediment: microbiological and biogeochemical interactions. In: Kristensen E, Haese RR, Kostka JE, Eds. *Interactions between macro- and microorganisms in marine sediments*. Washington: American Geophysical Union.
- Lancelot C, Spitz Y, Gypens N, Ruddick K, Becquevort S, Rousseau V, Lacroix G, Billen G. 2005. Modelling diatom and Phaeocystis blooms and nutrient cycles in the Southern Bight of the North Sea: the MIRO model. *Mar Ecol Prog Ser* 289:63–78.
- Maire O, Duchene JC, Gremare A, Malyuga VS, Meysman FJR. 2007. A comparison of sediment reworking rates by the surface deposit-feeding bivalve *Abra ovata* during summertime and wintertime, with a comparison between two models of sediment reworking. *J Exp Mar Biol Ecol* 343:21–36.
- Malkin SY, Rao AMF, Seitaj D, Vasquez-Cardenas D, Zetsche EM, Hidalgo-Martinez S, Boschker HTS, Meysman FJR. Accepted. Natural occurrence of microbial sulphur oxidation by long-range electron transport in the seafloor. *ISME J*.
- Marcus NH, Boero F. 1998. Minireview: the importance of benthic–pelagic coupling and the forgotten role of life cycles in coastal aquatic systems. *Limnol Ocean* 43:763–8.
- Mermillod-Blondin F, Rosenberg R, Francois-Carcaillet F, Norling K, Mauclaire L. 2004. Influence of bioturbation by three benthic infaunal species on microbial communities and biogeochemical processes in marine sediment. *Aquat Microb Ecol* 36:271–84.
- Mermillod-Blondin F, François-Carcaillet F, Rosenberg R. 2005. Biodiversity of benthic invertebrates and organic matter processing in shallow marine sediments: an experimental study. *J Exp Mar Biol Ecol* 315:187–209.
- Meysman FJ, Middelburg JJ, Heip CH. 2006. Bioturbation: a fresh look at Darwin's last idea. *Trends Ecol Evol* 21:688–95.
- Michaud E, Desrosiers G, Mermillod-Blondin F, Sundby B, Stora G. 2005. The functional group approach to bioturbation: the effects of biodiffusers and gallery-diffusers of the *Macoma balthica* community on sediment oxygen uptake. *J Exp Mar Biol Ecol* 326:77–88.

- Na T, Gribsholt B, Galaktionov OS, Lee T, Meysman FJR. 2008. Influence of advective bio-irrigation on carbon and nitrogen cycling in sandy sediments. *J Mar Res* 66:691–722.
- Nielsen LP, Risgaard-Petersen N, Fossing H, Christensen PB, Sayama M. 2010. Electric currents couple spatially separated biogeochemical processes in marine sediment. *Nature* 463:1071–4.
- Norling K, Rosenberg R, Hulth S, Gremare A, Bonsdorff E. 2007. Importance of functional biodiversity and species-specific traits of benthic fauna for ecosystem functions in marine sediment. *Mar Ecol Prog Ser* 332:11–23.
- Parsons TR, Maita Y, Lalli CM. 1984. A manual of chemical and biological methods for seawater analysis. New York: Pergamon Press.
- Pede A. 2012. Diversity and dynamics of protist communities in subtidal North Sea sediments in relation to metal pollution and algal bloom deposition.
- Pelegri SP, Nielsen LP, Blackburn TH. 1994. Denitrification in estuarine sediment stimulated by the irrigation activity of the amphipod *Corophium voluitor*. *Mar Ecol Prog Ser* 105:285–90.
- Pinheiro JC, Bates D. 2009. Mixed-effects models in S and S-PLUS. New York: Springer.
- Provoost P, Braeckman U, Vanaverbeke J, Middelburg JJ, Soetaert K. 2013. Benthic oxygen consumption and benthic–pelagic coupling at a shallow station in the Southern North Sea. *Estuar Coast Shelf Sci* 120:1–11.
- Queirós AM, Birchenough SNR, Bremner J, Godbold JA, Parker RE, Romero-Ramirez A, Reiss H, Solan M, Somerfield PJ, Van Colen C, Van Hoey G, Widdicombe S. 2013. A bioturbation classification of European marine infaunal invertebrates. *Ecol Evol* 3:3958–85.
- Raffaelli DG. 2006. Biodiversity and ecosystem functioning: issues of scale and trophic complexity. *Mar Ecol Prog Ser* 311:285–94.
- Rasheed M, Badran MI, Huettel M. 2003. Influence of sediment permeability and mineral composition on organic matter degradation in three sediments from the Gulf of Aqaba, Red Sea. *Estuar Coast Shelf Sci* 57:369–84.
- Risgaard-Petersen N, Revil A, Meister P, Nielsen LP. 2012. Sulfur, iron-, and calcium cycling associated with natural electric currents running through marine sediment. *Geochim Cosmochim Acta* 92:1–13.
- Rousseau V, Leynaert A, Daoud N, Lancelot C. 2002. Diatom succession, silicification and silicic acid availability in Belgian coastal waters (Southern North Sea). *Mar Ecol Prog Ser* 236:61–73.
- Rudnick DT. 1989. Time lags between the deposition and meiobenthic assimilation of phytodetritus. *Mar Ecol Prog Ser* 50:231–40.
- Rusch A, Forster S, Huettel M. 2001. Bacteria, diatoms and detritus in an intertidal sandflat subject to advective transport across the water-sediment interface. *Biogeochemistry* 55:1–27.
- Rysgaard S, Christensen PB, Nielsen LP. 1995. Seasonal variation in nitrification and denitrification in estuarine sediment colonized by benthic microalgae and bioturbating infauna. *Mar Ecol Prog Ser* 126:111–21.
- Seitzinger SP. 1988. Denitrification in freshwater and coastal marine ecosystems: ecological and geochemical significance. *Limnol Ocean Methods* 33:702–24.
- Smith SV, Hollibaugh JT. 1993. Coastal metabolism and the oceanic organic carbon balance. *Rev Geophys* 31:75–89.
- Soetaert K, Middelburg JJ. 2009. Modeling eutrophication and oligotrophication of shallow-water marine systems: the importance of sediments under stratified and well-mixed conditions. *Eutrophication Coast Ecosyst* 207:239–54.
- Soetaert K, Herman PMJ, Middelburg JJ, Heip C, Smith CL, Tett P, Wild-Allen K. 2001. Numerical modelling of the shelf break ecosystem: reproducing benthic and pelagic measurements. *Deep Sea Res II* 48:3141–77.
- Soetaert K, Van den Meersche K, van Oevelen D. 2009. LimSolve: solving linear inverse models. R Package Version 1. <http://cran.r-project.org/web/packages/limSolve/>. Accessed 03 July 2013.
- Solan M, Cardinale BJ, Downing AL, Engelhardt KAM, Ruesink JL, Srivastava DS. 2004. Extinction and ecosystem function in the marine benthos. *Science* 306:1177–80.
- Solan M, Scott F, Dulvy NK, Godbold JA, Parker R. 2012. Incorporating extinction risk and realistic biodiversity futures: implementation of trait-based extinction scenarios. *Marine biodiversity and ecosystem functioning: frameworks, methodologies, and integration*. Oxford: Oxford University Press. pp 127–48.
- Teal LR, Parker ER, Solan M. 2010. Sediment mixed layer as a proxy for benthic ecosystem process and function. *Mar Ecol Prog Ser* 414:27–40.
- Teal LR, Parker ER, Solan M. 2013. Coupling bioturbation activity to metal (Fe and Mn) profiles in situ. *Biogeosciences* 10:2365–78.
- Thomas H, Schiettecatte LS, Suykens K, Koné YJM, Shadwick EH, Prowe F, Bozec Y, de Baar HJW, Borges AV. 2009. Enhanced ocean carbon storage from anaerobic alkalinity generation in coastal sediments. *Biogeosciences* 6:267–74.
- Underwood AJ. 1997. Experiments in ecology: their logical design and interpretation using analysis of variance. Cambridge: Cambridge University Press.
- Van Colen C, Rossi F, Montserrat F, Andersson M, Gribsholt B, Herman P, Degraer S, Vincx M, Ysebaert T, Middelburg J. 2012. Organism–sediment interactions govern post-hypoxia recovery of ecosystem functioning. *PLoS ONE* 7(11): e49795.
- Van Hoey G, Degraer S, Vincx M. 2004. Macrobenthic community structure of soft-bottom sediments at the Belgian Continental Shelf. *Estuar Coast Shelf Sci* 59:599–613.
- Van Hoey G, Pecceu E, Vanaverbeke J, Hostens K, Vincx M. 2009. Macrobenthos monitoring on the Belgian Part of the North Sea in the framework of the OSPAR eutrophication assessment (EUTROF). Ilvo Report, p 50.
- Verfaillie E, Van Lancker V, Van Meirvenne M. 2006. Multivariate geostatistics for the predictive modelling of the surficial sand distribution in shelf seas. *Cont Shelf Res* 26:2454–68.
- Vitousek PM, Aber JD, Howarth RW, Likens GE, Matson PA, Schindler DW, Schlesinger WH, Tilman DG. 1997. Human alteration of the global nitrogen cycle: sources and consequences. *Ecol Appl* 7:737–50.
- Waldbusser GG, Marinelli RL, Whitlatch RB, Visscher PT. 2004. The effects of infaunal biodiversity on biogeochemistry of coastal marine sediments. *Limnol Ocean* 49:1482–92.
- Wentworth CK. 1922. A scale of grade and class terms for clastic sediments. *J Geol* 30:377–92.
- Wenzhöfer F, Glud RN. 2002. Benthic carbon mineralization in the Atlantic: a synthesis based on in situ data from the last decade. *Deep Sea Res I* 49:1255–79.

U. Braeckman and others

- West B, Welch KB, Galecki AT. 2006. Linear mixed models: a practical guide using statistical software. Boca Raton: Taylor & Francis.
- Wilson AM, Huettel M, Klein S. 2008. Grain size and depositional environment as predictors of permeability in coastal marine sands. *Estuar Coast Shelf Sci* 80(1):193–9.
- Wollast R. 1998. Evaluation and comparison of the global carbon cycle in the coastal zone and in the open ocean. *The Sea* 10:213–52.
- Wright SW, Jeffrey SW. 1997. High-resolution HPLC system for chlorophylls and carotenoids of marine phytoplankton. In: Jeffrey SW, Mantoura RFC, Wright SW, Eds. *Phytoplankton pigments in oceanography: guidelines to modern methods*. Paris: UNESCO. p 327–41.
- Yingst JY, Rhoads DC. 1980. The role of bioturbation in the enhancement of bacterial growth rates in marine sediments. In: Tenore, K.R. et al. Ed. *Marine Benthic Dynamics: 11th Belle W. Baruch symposium in marine science*, Georgetown (SC) April 1979. The Belle W. Baruch Library in Marine Science, pp 407–21.
- Zuur A, Ieno EN, Walker N. 2009. *Mixed effects models and extensions in ecology with R*. New York: Springer.